ESR Line Shapes for Triplets Undergoing Slow Rotational Reorientation*

JACK H. FREED, GERALD V. BRUNO, AND CARL POLNASZEK†
Department of Chemistry, Cornell University, Ithaca, New York 14850
(Received 27 July 1971)

The stochastic Liouville method is applied to analyze the general problem of unsaturated ESR line shapes for triplets undergoing rotational diffusion. Detailed line shape simulations are obtained for the cases of high-, low-, and zero-field resonance, large or small values of an axially symmetric zero-field splitting, and slow through fast rotational diffusion. It is shown how all these parameters can have profound effects on the observed ESR spectra.

I. INTRODUCTION

In a recent study, Norris and Weissman[1] examined the line shapes of triplet molecules tumbling slowly in viscous media. They were able to show that their spectra agreed favorably with what was predicted for small diffusivelike reorientational jumps as compared to spectra predicted for large reorientations (i.e., equal conditional probabilities for reorientation by any angle). Their work, then, suggests the possible value which such studies of triplet line shapes may have.

Because of the small zero-field splitting of their triplets ($D\sim100$ G), Norris and Weissman were able to successfully use the secular approximation to greatly simplify the calculation of their predicted spectra by finite difference techniques. More recently, Sillescu[2] has used a related approach to discuss secular ESR line shapes for slow tumbling.

Given that such studies can be of considerable interest for the study of molecular motion, it would clearly be valuable to be able to predict line shapes in the more general cases when the secular approximation is no longer valid. Even for the triplets studies by Norris and Weissman, the neglect of nonsecular terms precluded the possibility of their utilizing the $\Delta m=2$ transition. The problem of ESR (doublet) line shapes has already been discussed by Freed, Bruno, and Polnaszek[3] in recent work. The method employed in I was based on Kubo's stochastic Liouville approach.[4] An equation of motion for the spin-density matrix is written in terms of both its spin and orientational-diffusion dependence.[3] Rapidly converging steady-state solutions are then obtained by means of expansions in eigenfunctions of the Markovian-diffusion operator. In the present work, we apply this approach to the problem of triplet line shapes.

Perhaps the main difference between the triplet and the usual free radical doublet problem is that the triplet zero-field splitting is not, in general, small compared to the Zeeman term. Hence, high-field approximations need no longer be valid. We, therefore, must adopt an approach which applies for all values of the Zeeman field. This was not the case in I, where the density matrix approach, useful for discussing both line shapes and saturation phenomena, requires modification when high-field approximations do not apply. This problem is a difficult one, and is treated rigorously by Bloch[5] and Abragam[6] only for the case of a simple line. They show that the modified-Bloch equations for low fields,[6] wherein the susceptibility is proportional to ω, the radio frequency, rather than ω_0, the Larmour frequency, apply at least in special cases. By means of a linear response approach, wherein we forego any description of saturation effects, it is possible to obtain fundamentally sound descriptions of the line shapes without such problems. Thus, we treat the triplet line shape problem from this point of view, which is also closer to Kubo's original treatment of the stochastic Liouville method.[4a]

We also examine the characteristics of zero-field and low-field triplet line shapes.

II. THEORY

A. Formulation

We start with the general expression for the imaginary part of the magnetic susceptibility resulting from a very weak rf field of frequency $\omega/2\pi$ being applied to the system[7,8]

$$\chi_{\alpha\alpha}''(\omega)=\frac{\omega}{2NkT}\int_0^\infty (e^{i\omega t}+e^{-i\omega t})\ \mathrm{Tr}[M_\alpha(t)M_\alpha]dt. \quad (1)$$

The perturbation of the spins by the rf field is given by

$$\epsilon(t)=M_\alpha B_1\cos\omega t, \quad (2)$$

i.e., an oscillating field along the $\alpha=x$, y, or z direction. We shall assume an essentially isotropic g value and an ensemble of noninteracting triplets, so that

$$\mathrm{Tr}[M_\alpha(t)M_\alpha]=\mathfrak{N}\gamma_e^2\ \mathrm{Tr}[S_\alpha(t)S_\alpha], \quad (1')$$

where $\mathfrak{N}$ is the concentration of triplets, γ_e is the gyromagnetic factor, M_α is the operator for the αth component of the magnetization of the sample, and S_α the corresponding spin operator. Also,

$$S_\alpha(t)=\exp(i\mathcal{H}t)S_\alpha\exp(-i\mathcal{H}t), \quad (3)$$

N is the number of eigenstates of the Hamiltonian $\hbar\mathcal{H}$ of the system [in the absence of $\epsilon(t)$], and Eq. (1) is expressed in the high temperature approximation $[(\hbar\mathcal{H}/kT)\ll 1]$.

We now separate $\mathcal{H}$ into

$$\mathcal{H}=\mathcal{H}_z+\mathcal{H}_1(\Omega),$$

where $\mathcal{H}_z$ is the Zeeman part of the Hamiltonian and $\mathcal{H}_1(\Omega)$ contains the orientation dependent zero-field splitting terms. Here, $\mathcal{H}_1(\Omega)$ need not be small compared to $\mathcal{H}_z$. In the presence of random motion of the triplets, $\mathcal{H}_1(\Omega)$ becomes a random function of time. We assume that the motional process can be described as a stationary Markoff process. It then follows that an appropriate ensemble average operator $S_\alpha(\Omega, t)$ obeys the stochastic Liouville equation of motion,[3,4]

$$(\partial/\partial t)S_\alpha(\Omega, t)=i\mathcal{H}^x S_\alpha(\Omega, t)-\Gamma_\Omega S_\alpha(\Omega, t), \quad (4)$$

where $A^xB\equiv[A, B]$ with initial condition (for isotropic distribution of orientations)

$$S_\alpha(\Omega, 0)=S_\alpha(0). \quad (5)$$

Here Γ_Ω is the stationary Markovian operator which satisfies the differential equation

$$(\partial/\partial t)P(\Omega, t)=-\Gamma_\Omega P(\Omega, t), \quad (6)$$

where $P(\Omega, t)$ is the probability of finding a molecule at the particular orientation Ω at time t. Let

$$S_\alpha(s)\equiv\int_0^\infty e^{-st}S_\alpha(t)\,dt \quad (7)$$

be the Laplace transform of $S_\alpha(t)$. Then Eq. (4) with Eq. (5) may be transformed to

$$(S-i\mathcal{H}^x+\Gamma_\Omega)S_\alpha(s, \Omega)=S_\alpha(0). \quad (8)$$

Now, in Eq. (1′), the trace over orientational degrees of freedom is replaced by a classical average,

$$\langle S_\alpha(t)S_\alpha\rangle_{Av}\equiv\int d\Omega P_0(\Omega)S_\alpha(t, \Omega)S_\alpha=\langle S_\alpha(t)\rangle_{Av}S_\alpha, \quad (9)$$

where $P_0(\Omega)$ is the equilibrium distribution of orientations obeying

$$\Gamma P_0(\Omega)=0. \quad (10)$$

It follows from Eqs. (7) and (9) that the susceptibility, Eq. (1), may be rewritten as

$$\chi''(\omega)=(\mathfrak{N}\gamma_e^2\omega/2NkT)\times\mathrm{Tr}[\{\langle S_\alpha(i\omega)\rangle_{Av}+\langle S_\alpha(-i\omega)\rangle_{Av}\}S_\alpha], \quad (11)$$

where $S_\alpha(\pm i\omega)$ are the Laplace transforms of the spin operator with $S=\pm i\omega$, and the trace is now only over spin degrees of freedom. The plus and minus signs are found to correspond to the two counterrotating components of the rf field. Note that it follows from Eqs. (7) and (3), the Hermiticity of $S_\alpha(t)$, and the fact that Γ_Ω is a real operator independent of spin, that

$$S_\alpha(i\omega)^\dagger=S_\alpha(-i\omega), \quad (11')$$

where the dagger indicates Hermitian conjugate. Thus we require $\langle S_\alpha(s)\rangle_{Av}$ given by

$$\langle S_\alpha(\Omega, s)\rangle_{Av}=\langle[s-i\mathcal{H}^x+\Gamma_\Omega]^{-1}S_\alpha\rangle_{Av}=\int d\Omega P_0(\Omega)[s-i\mathcal{H}^x+\Gamma_\Omega]^{-1}S_\alpha. \quad (12)$$

The method of solution is to expand $S_\alpha(\Omega, s)$ in a complete set of orthogonal eigenfunctions of Γ_Ω, i.e., $G_m(\Omega)$, with eigenvalues E_m

$$S_\alpha(\Omega, \pm i\omega)=\sum_m a_{\alpha,m}(\pm\omega)G_m(\Omega), \quad (13)$$

where $a_{m,\alpha}(\omega)$ are still operators in spin space. It then follows from Eq. (11′) that

$$a_m(\omega)=a_m^\dagger(-\omega)N_m^{-1}\sum_{m'}\int d\Omega G_m^*(\Omega)G_{m'}^*(\Omega), \quad (14)$$

where

$$N_m=\int d\Omega G_m^*(\Omega)G_m(\Omega). \quad (14')$$

Clearly, from Eqs. (7), (9), and (13),

$$\langle S_\alpha(\Omega, \pm i\omega)\rangle_{Av}=a_{\alpha,0}(\pm\omega) \quad (15)$$

when we take $P_0\propto G_0(\Omega)\equiv 1$, i.e., an isotropic *a priori* distribution of orientations.

B. Triplets $B_1\perp B_0$

Here, we are interested in S_x. Now, the nonzero matrix elements of S_x are $\langle\pm\mid S_x\mid 0\rangle=\langle 0\mid S_x\mid\pm\rangle=\sqrt{2}/2$. It thus follows from Eqs. (11), (11′), and (15) that

$$\chi''(\omega)=(\sqrt{2}\omega/2NkT)\mathfrak{N}\gamma_e^2\,\mathrm{Re}[\langle-\mid a_{x,0}(\pm\omega)\mid 0\rangle+\langle 0\mid a_{x,0}(\pm\omega)\mid+\rangle], \quad (16)$$

where the $a_{x,0}(\pm\omega)$ terms imply that the effects of both the rotating and counterrotating components are to be added. Also, we have, for the zero-field terms

$$\mathcal{H}_1=\sum_{m'}\{6^{-1/2}D\mathfrak{D}_{0,m'}^2(\Omega)+(E/2)[\mathfrak{D}_{2,m'}^2(\Omega)+\mathfrak{D}_{-2,m'}^2(\Omega)]\}A^{2,m'}, \quad (17)$$

where $A^{2,0}=6^{1/2}(S_z^2-\frac{1}{3}S^2)$,

$$A^{2,\pm 1}=\mp(S_\pm S_z+S_zS_\pm),$$
$$A^{2,\pm 2}=S_\pm^2. \quad (18)$$

Here, Ω represents the Euler angles for the transformation from molecular to space fixed axes.[9] For a rotational-motion modulation of $\mathcal{H}_1(\Omega)$, we shall employ the solutions for isotropic rotational diffusion. That is, we have $G_m\rightarrow\mathfrak{D}_{KM}^L(\Omega)$, the Wigner rotation matrices, with

eigenvalues $E_m=E_{L,K,M}=RL(L+1)$, with R the isotropic rotational diffusion coefficient. The case of anisotropic rotational diffusion is also readily handled,[9,10] but in this work we mainly confine our examples to the isotropic case. By means of the methods of I, Eqs. (8) and (13) yield sets of coupled differential equations for matrix elements of the coefficients $a_{K,M}{}^{L}(\pm\omega)$. We introduce the modified coefficients[11]

$$C_{KM}{}^{L}(\pm\omega)=\pm i(-)^{K-M}a_{-K-M}{}^{L*}(\mp\omega) \qquad (19)$$

and abbreviate the matrix elements of the $C_{K,M}{}^{L}(\pm\omega)$ as

$$\begin{aligned}
\langle -\,|\,C\,|\,0\rangle &= C(1), & \langle 0\,|\,C\,|\,-\rangle &= C(-1),\\
\langle 0\,|\,C\,|\,1\rangle &= C(2), & \langle 1\,|\,C\,|\,0\rangle &= C(-2),\\
\langle -1\,|\,C\,|\,1\rangle &= C(3), & \langle 1\,|\,C\,|\,-1\rangle &= C(-3),\\
\langle -1\,|\,C\,|\,-1\rangle &= C(a), & \langle 0\,|\,C\,|\,0\rangle &= C(b),\\
\multicolumn{4}{c}{\langle 1\,|\,C\,|\,1\rangle = C(c).} \qquad (20)
\end{aligned}$$

We also let $P\equiv D/6^{1/2}$ and set $E=0$. The coupled equations for the $C_{K,M}{}^{L}(\omega,i)$, where ω will be dropped for convenience, are, in terms of the $3j$ symbols:

$$(2L+1)^{-1}[(\omega-\omega_0)-iRL(L+1)]C_{0,0}{}^{L}(1)+P\sum_{L'}\begin{pmatrix}L&2&L'\\0&0&0\end{pmatrix}\Bigg[6^{1/2}\begin{pmatrix}L&2&L'\\0&0&0\end{pmatrix}C_{0,0}{}^{L'}(1)$$

$$+\sqrt{2}\begin{pmatrix}L&2&L'\\0&-1&1\end{pmatrix}\{C_{0,1}{}^{L'}(a)-C_{0,1}{}^{L'}(b)+C_{0,-1}{}^{L'}(3)\}+2\begin{pmatrix}L&2&L'\\0&-2&2\end{pmatrix}C_{0,2}{}^{L'}(-2)\Bigg]=\frac{\sqrt{2}}{2}\delta(L,0), \qquad (21a)$$

$$(2L+1)^{-1}[(\omega-\omega_0)-iRL(L+1)]C_{0,0}{}^{L}(2)+P\sum_{L'}\begin{pmatrix}L&2&L'\\0&0&0\end{pmatrix}\Bigg[-6^{1/2}\begin{pmatrix}L&2&L'\\0&0&0\end{pmatrix}C_{0,0}{}^{L'}(2)$$

$$+\sqrt{2}\begin{pmatrix}L&2&L'\\0&-1&1\end{pmatrix}\{-C_{0,1}{}^{L'}(b)+C_{0,1}{}^{L'}(c)+C_{0,-1}{}^{L'}(3)\}-2\begin{pmatrix}L&2&L'\\0&-2&2\end{pmatrix}C_{0,2}{}^{L'}(-1)\Bigg]=\tfrac{1}{2}\sqrt{2}\delta(L,0), \qquad (21b)$$

$$(2L+1)^{-1}[\omega-iRL(L+1)]C_{0,1}{}^{L}(a)+P\sum_{L'}\begin{pmatrix}L&2&L'\\0&0&0\end{pmatrix}\Bigg[\sqrt{2}\begin{pmatrix}L&2&L'\\-1&1&0\end{pmatrix}C_{0,0}{}^{L'}(1)$$

$$+2\begin{pmatrix}L&2&L'\\-1&2&-1\end{pmatrix}C_{0,-1}{}^{L'}(3)-2\begin{pmatrix}L&2&L'\\-1&-2&3\end{pmatrix}C_{0,3}{}^{L'}(-3)+\sqrt{2}\begin{pmatrix}L&2&L'\\-1&-1&2\end{pmatrix}C_{0,2}{}^{L'}(-1)\Bigg]=0, \qquad (21c)$$

$$(2L+1)^{-1}[\omega-iRL(L+1)]C_{0,1}{}^{L}(b)+P\sum_{L'}\begin{pmatrix}L&2&L'\\0&0&0\end{pmatrix}\Bigg[-\sqrt{2}\begin{pmatrix}L&2&L'\\-1&1&0\end{pmatrix}\{C_{0,0}{}^{L'}(1)+C_{0,0}{}^{L'}(2)\}$$

$$-\sqrt{2}\begin{pmatrix}L&2&L'\\-1&-1&2\end{pmatrix}\{C_{0,2}{}^{L'}(-1)+C_{0,2}{}^{L'}(-2)\}\Bigg]=0, \qquad (21d)$$

$$(2L+1)^{-1}[\omega-iRL(L+1)]C_{0,1}{}^{L}(c)+P\sum_{L'}\begin{pmatrix}L&2&L'\\0&0&0\end{pmatrix}\Bigg[\sqrt{2}\begin{pmatrix}L&2&L'\\-1&1&0\end{pmatrix}C_{0,0}{}^{L'}(2)$$

$$-2\begin{pmatrix}L&2&L'\\-1&2&-1\end{pmatrix}C_{0,-1}{}^{L'}(3)+2\begin{pmatrix}L&2&L'\\-1&-2&3\end{pmatrix}C_{0,3}{}^{L'}(-3)+\sqrt{2}\begin{pmatrix}L&2&L'\\-1&-1&2\end{pmatrix}C_{0,2}{}^{L'}(-2)\Bigg]=0, \qquad (21e)$$

$$(2L+1)^{-1}[(\omega-2\omega_0)-iRL(L+1)]C_{0,-1}{}^{L}(3)+P\sum_{L'}\begin{pmatrix}L&2&L'\\0&0&0\end{pmatrix}\Bigg[\sqrt{2}\begin{pmatrix}L&2&L'\\1&-1&0\end{pmatrix}\{C_{0,0}{}^{L'}(1)+C_{0,0}{}^{L'}(2)\}$$

$$+2\begin{pmatrix}L&2&L'\\1&-2&1\end{pmatrix}\{C_{0,1}{}^{L'}(a)-C_{0,1}{}^{L'}(c)\}\Bigg]=0, \qquad (21f)$$

$$(2L+1)^{-1}[(\omega+\omega_0)-iRL(L+1)]C_{0,2}{}^{L}(-1)+P\sum_{L'}\begin{pmatrix}L&2&L'\\0&0&0\end{pmatrix}\Bigg[-6^{1/2}\begin{pmatrix}L&2&L'\\-2&0&2\end{pmatrix}C_{0,2}{}^{L'}(-1)$$

$$-2\begin{pmatrix}L&2&L'\\-2&2&0\end{pmatrix}C_{0,0}{}^{L'}(2)+\sqrt{2}\begin{pmatrix}L&2&L'\\-2&1&1\end{pmatrix}\{C_{0,1}{}^{L'}(a)-C_{0,1}{}^{L'}(b)\}+\sqrt{2}\begin{pmatrix}L&2&L'\\-2&-1&3\end{pmatrix}C_{0,3}{}^{L'}(-3)\Bigg]=0, \tag{21g}$$

$$(2L+1)^{-1}[(\omega+\omega_0)-iRL(L+1)]C_{0,2}{}^{L}(-2)+P\sum_{L'}\begin{pmatrix}L&2&L'\\0&0&0\end{pmatrix}\Bigg[6^{1/2}\begin{pmatrix}L&2&L'\\-2&0&2\end{pmatrix}C_{0,2}{}^{L'}(-2)$$

$$+2\begin{pmatrix}L&2&L'\\-2&2&0\end{pmatrix}C_{0,0}{}^{L'}(1)+\sqrt{2}\begin{pmatrix}L&2&L'\\-2&1&1\end{pmatrix}\{C_{0,1}{}^{L'}(c)-C_{0,1}{}^{L'}(b)\}+\sqrt{2}\begin{pmatrix}L&2&L'\\-2&-1&3\end{pmatrix}C_{0,3}{}^{L'}(-3)\Bigg]=0, \tag{21h}$$

$$(2L+1)^{-1}[(\omega+2\omega_0)-iRL(L+1)]C_{0,3}{}^{L}(-3)+P\sum_{L'}\begin{pmatrix}L&2&L'\\0&0&0\end{pmatrix}\Bigg[2\begin{pmatrix}L&2&L'\\-3&2&1\end{pmatrix}\{C_{0,1}{}^{L'}(c)-C_{0,1}{}^{L'}(a)\}$$

$$+\sqrt{2}\begin{pmatrix}L&2&L'\\-3&1&2\end{pmatrix}\{C_{0,2}{}^{L'}(-1)+C_{0,2}{}^{L'}(-2)\}\Bigg]=0. \tag{21i}$$

The equations for $C_{K,M}{}^{L}(-\omega, i)$ are obtained by letting $\omega\rightarrow-\omega$ and $C_{K,M}{}^{L}(\omega, i)\rightarrow-C_{KM}{}^{L}(-\omega, i)$ in Eqs. (21). From Eqs. (16) and (19),

$$\chi''(\omega)=(\sqrt{2}\omega/2NkT)\mathfrak{N}\gamma_e{}^2\,\mathrm{Im}[\pm C_{0,0}{}^{0}(\pm\omega, 1)\pm C_{0,0}{}^{0}(\pm\omega, 2)]. \tag{22}$$

In Eqs. (21) we can introduce rotationally invariant width terms $T_2{}^{-1}(i)$ where $i=1$, 2, or 3 for the ±1, ±2, and ±3 transitions simply by letting $RL(L+1)\rightarrow T_2{}^{-1}(i)+RL(L+1)$. We otherwise neglect other relaxation mechanisms (e.g., rotational modulation of the g tensor) and other sources of broadening assumed to be small.

Similarly, one can introduce rotationally invariant relaxation transitions between the $+1$, 0, and -1 levels, but we assume the latter are small. Equations (21) apply for L even, but only a and b for $L\geqq0$. All others are for $L>0$. When the equations are truncated for $L>n$, the dimension of the coupled equations is $(2+\frac{9}{2}n)$. The coupled equations needed for $E\neq0$ can readily be written down,[12] but are somewhat more complicated than Eq. (21), so they are not reproduced here.

C. Triplets $B_1 \,||\, B_0$

Here, we have $\langle+\,|\,S_z\,|\,+\rangle=-\langle-\,|\,S_z\,|\,-\rangle=1$, and we obtain

$$\begin{aligned}\chi''(\omega)&=(\mathfrak{N}\gamma_e{}^2\omega/NkT)\,\mathrm{Re}[\langle+\,|\,a_{z,0}(-\omega)\,|\,+\rangle-\langle-\,|\,a_{z,0}(-\omega)\,|\,-\rangle]\\&=(\mathfrak{N}\gamma_e{}^2\omega/NkT)\,\mathrm{Im}[C_{0,0}{}^{0}(\omega, a)-C_{0,0}{}^{0}(\omega, c)].\end{aligned} \tag{23}$$

The coupled equations needed to obtain these coefficients are

$$(2L+1)^{-1}[\omega-iRL(L+1)]C_{0,0}{}^{L}(a)+P\sum_{L'}\begin{pmatrix}L&2&L'\\0&0&0\end{pmatrix}\Bigg[-\sqrt{2}\begin{pmatrix}L&2&L'\\0&1&-1\end{pmatrix}\{C_{0,-1}{}^{L'}(1)+C_{0,1}{}^{L'}(-1)\}$$

$$-2\begin{pmatrix}L&2&L'\\0&2&-2\end{pmatrix}\{C_{0,-2}{}^{L'}(3)-C_{0,2}{}^{L'}(-3)\}\Bigg]=\delta(L, 0), \tag{24a}$$

$$(2L+1)^{-1}[\omega-iRL(L+1)]C_{0,0}{}^{L}(b)+P\sum_{L'}\begin{pmatrix}L&2&L'\\0&0&0\end{pmatrix}\Bigg[\sqrt{2}\begin{pmatrix}L&2&L'\\0&1&-1\end{pmatrix}$$

$$\times\{C_{0,-1}{}^{L'}(1)+C_{0,1}{}^{L'}(-1)+C_{0,-1}{}^{L'}(2)+C_{0,1}{}^{L'}(-2)\}\Bigg]=0, \tag{24b}$$

$$(2L+1)^{-1}[\omega-iRL(L+1)]C_{0,0}{}^{L}(c)+P\sum_{L'}\begin{pmatrix}L & 2 & L'\\ 0 & 0 & 0\end{pmatrix}\Bigg[-\sqrt{2}\begin{pmatrix}L & 2 & L'\\ 0 & 1 & -1\end{pmatrix}\{C_{0,-1}{}^{L'}(2)+C_{0,1}{}^{L'}(-2)\}$$

$$+2\begin{pmatrix}L & 2 & L'\\ 0 & 2 & -2\end{pmatrix}\{C_{0,-2}{}^{L'}(3)-C_{0,2}{}^{L'}(-3)\}\Bigg]=-\delta(L,0), \quad (24c)$$

$$(2L+1)^{-1}[(\omega-\omega_0)-iRL(L+1)]C_{0,-1}{}^{L}(1)+P\sum_{L'}\begin{pmatrix}L & 2 & L'\\ 0 & 0 & 0\end{pmatrix}\Bigg[-6^{1/2}\begin{pmatrix}L & 2 & L'\\ 1 & 0 & -1\end{pmatrix}C_{0,-1}{}^{L'}(1)$$

$$-\sqrt{2}\begin{pmatrix}L & 2 & L'\\ 1 & -1 & 0\end{pmatrix}\{C_{0,0}{}^{L'}(a)-C_{0,0}{}^{L'}(b)\}-\sqrt{2}\begin{pmatrix}L & 2 & L'\\ 1 & 1 & -2\end{pmatrix}C_{0,-2}{}^{L'}(3)-2\begin{pmatrix}L & 2 & L'\\ 1 & -2 & 1\end{pmatrix}C_{0,1}{}^{L'}(-2)\Bigg]=0, \quad (24d)$$

$$(2L+1)^{-1}[(\omega-\omega_0)-iRL(L+1)]C_{0,-1}{}^{L}(2)+P\sum_{L'}\begin{pmatrix}L & 2 & L'\\ 0 & 0 & 0\end{pmatrix}\Bigg[6^{1/2}\begin{pmatrix}L & 2 & L'\\ 1 & 0 & -1\end{pmatrix}C_{0,-1}{}^{L'}(2)$$

$$+\sqrt{2}\begin{pmatrix}L & 2 & L'\\ 1 & -1 & 0\end{pmatrix}\{C_{0,0}{}^{L'}(b)-C_{0,0}{}^{L'}(c)\}-\sqrt{2}\begin{pmatrix}L & 2 & L'\\ 1 & 1 & -2\end{pmatrix}C_{0,-2}{}^{L'}(3)+2\begin{pmatrix}L & 2 & L'\\ 1 & -2 & 1\end{pmatrix}C_{0,1}{}^{L'}(-1)\Bigg]=0, \quad (24e)$$

$$(2L+1)^{-1}[(\omega-2\omega_0)-iRL(L+1)]C_{0,-2}{}^{L}(3)+P\sum_{L'}\begin{pmatrix}L & 2 & L'\\ 0 & 0 & 0\end{pmatrix}\Bigg[-\sqrt{2}\begin{pmatrix}L & 2 & L'\\ 2 & -1 & -1\end{pmatrix}\{C_{0,-1}{}^{L}(1)+C_{0,-1}{}^{L}(2)\}$$

$$-2\begin{pmatrix}L & 2 & L'\\ 2 & -2 & 0\end{pmatrix}\{C_{0,0}{}^{L'}(a)-C_{0,0}{}^{L'}(c)\}\Bigg]=0, \quad (24f)$$

$$(2L+1)^{-1}[(\omega+\omega_0)-iRL(L+1)]C_{0,1}{}^{L}(-1)+P\sum_{L'}\begin{pmatrix}L & 2 & L'\\ 0 & 0 & 0\end{pmatrix}\Bigg[6^{1/2}\begin{pmatrix}L & 2 & L'\\ -1 & 0 & 1\end{pmatrix}C_{0,1}{}^{L'}(-1)$$

$$-\sqrt{2}\begin{pmatrix}L & 2 & L'\\ -1 & 1 & 0\end{pmatrix}\{C_{0,0}{}^{L'}(a)-C_{0,0}{}^{L'}(b)\}-\sqrt{2}\begin{pmatrix}L & 2 & L'\\ -1 & -1 & 2\end{pmatrix}C_{0,2}{}^{L'}(-3)+2\begin{pmatrix}L & 2 & L'\\ -1 & 2 & -1\end{pmatrix}C_{0,-1}{}^{L'}(2)\Bigg]=0, \quad (24g)$$

$$(2L+1)^{-1}[(\omega+\omega_0)-iRL(L+1)]C_{0,1}{}^{L}(-2)+P\sum_{L'}\begin{pmatrix}L & 2 & L'\\ 0 & 0 & 0\end{pmatrix}\Bigg[-6^{1/2}\begin{pmatrix}L & 2 & L'\\ -1 & 0 & 1\end{pmatrix}C_{0,1}{}^{L}(-2)$$

$$+\sqrt{2}\begin{pmatrix}L & 2 & L'\\ -1 & 1 & 0\end{pmatrix}\{C_{0,0}{}^{L'}(b)-C_{0,0}{}^{L'}(c)\}-\sqrt{2}\begin{pmatrix}L & 2 & L'\\ -1 & -1 & 2\end{pmatrix}C_{0,2}{}^{L'}(-3)-2\begin{pmatrix}L & 2 & L'\\ -1 & 2 & -1\end{pmatrix}C_{0,-1}{}^{L'}(1)\Bigg]=0, \quad (24h)$$

$$(2L+1)^{-1}[(\omega+2\omega_0)-iRL(L+1)]C_{0,2}{}^{L}(-3)+P\sum_{L'}\begin{pmatrix}L & 2 & L'\\ 0 & 0 & 0\end{pmatrix}\Bigg[2\begin{pmatrix}L & 2 & L'\\ -2 & 2 & 0\end{pmatrix}\{C_{0,0}{}^{L'}(a)-C_{0,0}{}^{L'}(c)\}$$

$$-\sqrt{2}\begin{pmatrix}L & 2 & L'\\ -2 & 1 & 1\end{pmatrix}\{C_{0,1}{}^{L'}(-1)+C_{0,1}{}^{L'}(-2)\}\Bigg]=0. \quad (24i)$$

D. Perturbation Theory

There are two limiting cases in which Eqs. (21) and (24) may be solved more simply.

1. *High-Field Case*

Here, D, $6R \ll \omega_0$. A simple analysis of Eqs. (21) shows that one can neglect all terms on the rhs of Eq. (21a) not involving $C_{0,0}{}^L(1)$ provided L is not so large that $L(L+1)R \ll \omega_0$ is not fulfilled. In this approximation (the secular approximation), $C_{0,0}{}^0(1)$ couples only to the other $C_{0,0}{}^L(1)$, $L>0$. A similar simplified set of equations for the $C_{0,0}{}^L(2)$ is obtained from Eq. (21b). It is in this approximation that Norris and Weissman's calculations are valid.

In order to obtain the half-field transition in this approximation, it is necessary to use perturbation theory. Thus, the terms in Eqs. (21a) and (21b) which couple in $C_{K,M}{}^L(3)$ terms are used to mix in to second order in perturbation theory a small amount of half-field transition character. The perturbation method is similar to that discussed in paper I, Sec. IV. Equations (24) for the $B_1 \,||\, B_0$ case may be treated in a similar manner.

A more direct method which yields essentially the same result is obtained by first correcting the $|-\rangle$ and $|+\rangle$ states to first order in the perturbation Eq. (17) (let $E=0$). Then

$$|\pm'\rangle \cong |\pm\rangle \pm (\sqrt{2}\mathfrak{D}_{0,\mp 1}{}^2 P/\omega_0)|0\rangle \pm (\mathfrak{D}_{0,\mp 2}{}^2 P/\omega_0)|\mp\rangle, \tag{25}$$

and we otherwise neglect $\mathfrak{K}_1$ in the Hamiltonian except for the small energy corrections (to second order). The energies become $E_\pm \cong E_\pm{}' + 6^{1/2}\mathfrak{D}_{0,0}{}^2 P$, where $E_\pm{}'$ are

$$E_\pm{}' = \pm\omega_0 \pm 2(P^2/\omega_0)[(2/5) - (1/7)\mathfrak{D}_{0,0}{}^2 - (9/35)\mathfrak{D}_{0,0}{}^4]. \tag{26}$$

Now, from Eqs. (1) and (16) (but neglecting the nonresonant rotating component of the linear rf field), we have

$$\chi_\perp{}''(\omega) \cong \frac{\mathfrak{N}\gamma_e{}^2\omega}{NkT} \times \mathrm{Re}\int_0^\infty \langle\langle +'|S_x(t)|-'\rangle\langle -'|S_x(0)|+'\rangle\rangle_{\mathrm{Av}} e^{-i\omega t}dt$$

$$= \frac{\mathfrak{N}\gamma_e{}^2\omega}{NkT}\frac{P^2}{\omega_0}\mathrm{Re}\int_0^\infty dt e^{-i\omega t} \times \langle \exp(i2E_+{}'t)\mathfrak{D}_{0,-1}{}^{2*}(t)\mathfrak{D}_{0,-1}{}^2(0)\rangle_{\mathrm{Av}}, \tag{27}$$

where we have used Eqs. (25) and (26). When the second order energy corrections dependent on orientation are neglected, then we have

$$\langle \mathfrak{D}_{0,-1}{}^{2*}(t)\mathfrak{D}_{0,-1}{}^2(0)\rangle_{\mathrm{Av}} = \tfrac{1}{5}e^{-6Rt} \tag{28}$$

and

$$\chi_\perp{}''(\omega) \sim\sim \propto (P^2\omega/5\omega_0{}^2)\,\mathrm{Re}[(\omega - 2\omega_0{}') - i6R]^{-1} \tag{29}$$

or a simple Lorentzian of width $6R=\tau_R{}^{-1}$, where $2\omega_0{}' = 2\omega_0 + (4/15)(D^2/\omega_0)$, causing a small downfield shift. A more careful analysis shows that the downfield shift is $(2/7)\times(D^2/\omega_0)$. There is still a small residual orientation-dependent term from the second order energy, but it is found to average out when $D^2/\omega_0 R \ll 330$ with a negligible Lorentzian width component of $5.28\times 10^{-5}(D^4/\omega_0{}^2 R)$. This analysis is most conveniently performed by solving the first expression of Eq. (27) [with the approximations of Eqs. (25) and (26) for $\mathfrak{K}_1$] by utilizing the general method of Eqs. (7)–(9) and (13) and recognizing that, since the matrix elements of S_x as well as $S_x(t)$ are orientation dependent, both terms must be included in all averaging procedures.[13]

A similar perturbation analysis for $H_1 \,||\, H_0$ yields in the approximation of Eq. (29),

$$\chi_{||}{}''(\omega) = \chi_\perp{}''(\omega). \tag{30}$$

Note that, from the form of Eq. (29), the observed derivative linewidth of the half-field line in a field-swept experiment is given by

$$\delta = (2\gamma_e)^{-1}[(2/\sqrt{3})\{T_2{}^{-1} + 6R\}], \tag{31}$$

where $2\gamma_e$ is the "effective" gyromagnetic factor and $T_2{}^{-1}$ is the rotationally invariant width term.

2. *Fast Motional Case*

Here, $D \ll 6R$. This is the condition for conventional relaxation theory to apply. One obtains a single Lorentzian line at $\omega=\omega_0$ with[14]

$$T_2{}^{-1} = (\Delta^2/20)[3J(0) + 5J(\omega_0) + 2J(2\omega_0)], \tag{32}$$

where $\Delta^2 = 2(D^2/3 + E)$ and $J(\omega) = 12R/[(6R)^2 + \omega^2]$. This result can also be obtained from a perturbation analysis of Eqs. (21) using only terms up through $L=2$. Cases 1 and 2 are clearly not mutually exclusive.

E. Rigid Limit Spectra

The triplet spectra in the rigid limit were simulated essentially in the manner of Kottis and Lefebvre[15] and of Wasserman *et al.*[16] Several modifications, however, have been made which improve the efficiency of the program. First, the basis sets used may be written as[17]

$$|\Phi_m\rangle = \sum_{m'} \mathfrak{D}_{m'm}{}^1(\phi, \theta, 0)|m'\rangle, \tag{33}$$

where the $|\Phi_m\rangle$ are just the high-field spin functions and $|m'\rangle$ the functions quantitized in the molecular frame. This basis set leads to a real and symmetric matrix representation for the Hamiltonian when $E=0$.

The resonant fields B_θ are then obtained from

$$2(B_\theta{}^2 + \tfrac{1}{3}\hat{D}^2)^{1/2}\sin(V + n\pi/3) - (\omega/|\gamma_e|) = 0,$$

$$V = \tfrac{1}{3}\arccos\{[(27/2)B_\theta{}^2\hat{D}(\cos^2\theta - \tfrac{1}{3}) - \hat{D}^3] \times [27B_\theta{}^6 + 27B_\theta{}^4\hat{D}^2 + 9B_\theta{}^2\hat{D}^4 + \hat{D}^6]^{-1/2}\}, \tag{34}$$

where $n=1$ for a $\Delta m=2$ transition, and $n=2$, 3 for

TABLE I. A comparison of linewidths for the $\Delta_m=2$ transition as obtained from computer simulations and from perturbation analysis.

	D/R	Derivative linewidth in gauss: Computer simulation	Derivative linewidth in gauss: Perturbation result[c]	Position of absorption max. $\times 2$
(A) Small D [a]				
$B_1 \| B_0$	30	17.6	17.5	3 296 G
$B_1 \perp B_0$	30	17.5	17.5	3 296
$B_1 \| B_0$	100	5.4	5.5	3 296
$B_1 \perp B_0$	100	5.6	5.5	3 296
(B) Large D [b]				
$B_1 \| B_0$	40	145	132	2 924
$B_1 \perp B_0$	40	144	132	2 928
$B_1 \| B_0$	200	42.5	32.3	2 920
$B_1 \perp B_0$	200	42.5	32.3	2 894

[a] $B_0=3\,300$ G; $D/|\gamma_e|=150$ G; $T_2^{-1}/|\gamma_e|=(\sqrt{3}/2)$ 0.5 G.
[b] $B_0=3\,300$ G; $D/|\gamma_e|=1\,435$ G; $T_2^{-1}/|\gamma_e|=(\sqrt{3}/2)$ 15 G.
[c] Cf. Eq. (31).

$\Delta m=1$ transitions. Equation 34 results from solving the secular determinant for the eigenvalues and setting the difference equal to $|\omega/\gamma_e|$. Note that $\hat{D}=D/|\gamma_e|$. The eigenvalues are then given by

$$E_i=\tfrac{2}{3}(3B_\theta^2+\hat{D}^2)^{1/2}\cos(V+\tfrac{1}{3}k\pi), \qquad (35)$$

where $k=0$ for $i=1$, $k=4$ for $i=0$, and $k=2$ for $i=-1$. It is then a simple matter to solve for the eigenvectors $\Psi_i=\sum_m a_{im}\Phi_m$, from which real analytic expressions are obtained for the transition probabilities W_{ij}:

(1) B_1 parallel to B_0,

$$W_{ij}=[a_{i1}a_{j1}-a_{i-1}a_{j-1}]^2+\tfrac{1}{4}[a_{i0}(a_{j1}+a_{j-1}) -a_{j0}(a_{i1}+a_{i-1})]^2\cdot\sin^2\theta; \qquad (36a)$$

(2) B_1 perpendicular to B_0,

$$W_{ij}=[a_{i1}a_{j0}-a_{i0}a_{j-1}]^2+[a_{i0}a_{j1}-a_{i-1}a_{j0}]^2 -\tfrac{1}{4}[a_{i0}(a_{j1}+a_{j-1})-a_{j0}(a_{i1}+a_{i-1})]^2\sin^2\theta. \qquad (36b)$$

The integrations over all orientations are performed in the usual manner.

III. DISCUSSION OF RESULTS

The coupled equations were solved using Gaussian elimination with pivoting. Single precision was found sufficiently accurate (within 0.01% of double precision results). Diagonalization methods are not readily very convenient for field-swept simulations, because the $C_{KM}^L(\alpha)$, $\alpha=a$, b, or c have no dependence on ω_0 (which is varied over a wide range in a field-swept experiment), while the other $C_{KM}^L(i)$ have such explicit dependence. Thus, one cannot separate out ω_0 from the diagonalization, and repetitive diagonalizations would be required. For small relative variations in ω_0 or frequency-swept simulations, diagonalization methods are, of course, convenient.

While the same value of T_2^{-1} was used for all transitions in the results shown, it was found that only $T_2^{-1}(i)$ had any significant effect on the spectral line for the ith transition. The calculations were based on the triphenylene triplet, where $D/|\gamma_e|=1\,435$ G, and $E=0$. The calculations were of three types: (A) high-frequency, $\omega/|\gamma_e|\equiv B=3\,300$ G. (9.24 kMc/sec) and field sweep, (B) low-field, $B_0=\omega_0/|\gamma_e|=300$ G and frequency sweep, (C) zero-field and frequency sweep. However, these results scale for any triplet with $E=0$ provided the value of B or B_0 is chosen so (A) $D/\omega=0.43$, (B) $D/\omega_0=4.78$, (C) $\omega_0=0$. [E.g., for $D/|\gamma_e|=100$ G, we require (A) $B=230$ G, (B) $B_0=21$ G, (C) $B_0=0$.]

For case (A), the effects of the counterrotating field [the $C_{0,0}^0(-\omega, i)$ in Eq. (22)] were negligible. They were very important for the low field spectra.

A. High-Frequency and Field Sweep

The results for this case are given in Figs. 1–3. Figure 1 shows the results when $B_1\perp B_0$. As the rotational motion increases from the rigid limit, both the $\Delta m=1$ and 2 lines initially broaden. However, fast motion leads to a narrowing of the $\Delta m=1$ transition until it becomes Lorentzian with its absorption maximum at $B=3\,300$ G and width given by Eq. (32).

The broadening of the $\Delta m=2$ transition with increasing R is shown more clearly in Fig. 2. The derivative widths obtained in this figure are given in Table I, and are compared with the prediction of Eq. (31), even though the condition $D/\omega_0\ll 1$, required for the validity of this equation, is not fulfilled. The predicted widths are systematically low, although they are of the correct order. Also, the position of the absorption maximum is shifted significantly downfield. On the other hand, when spectra were computed with a small $D/|\gamma_e|=150$ G, then the agreement with Eq. (31) as given in Table I is seen to be very good. The small downfield shift of 2 G is also properly predicted by the perturbation analysis of Sec. II.D.

The $\Delta m=2$ transition for $B_1 \| B_0$ is shown in Fig. 3 and results also given in Table I. These results are very similar to what is obtained for the $B_1\perp B_0$ case.

B. Low Field and Frequency Sweep

The results for this case are given in Figs. 4 and 5, which show the $B_1\perp B_0$ and $B_1 \| B_0$ rf orientations, respectively. In both cases, as the motion starts, the rigid limit spectra occurring in the region of $\omega\sim D=1\,435$ G$\times|\gamma_e|$ are seen to broaden out. However, as

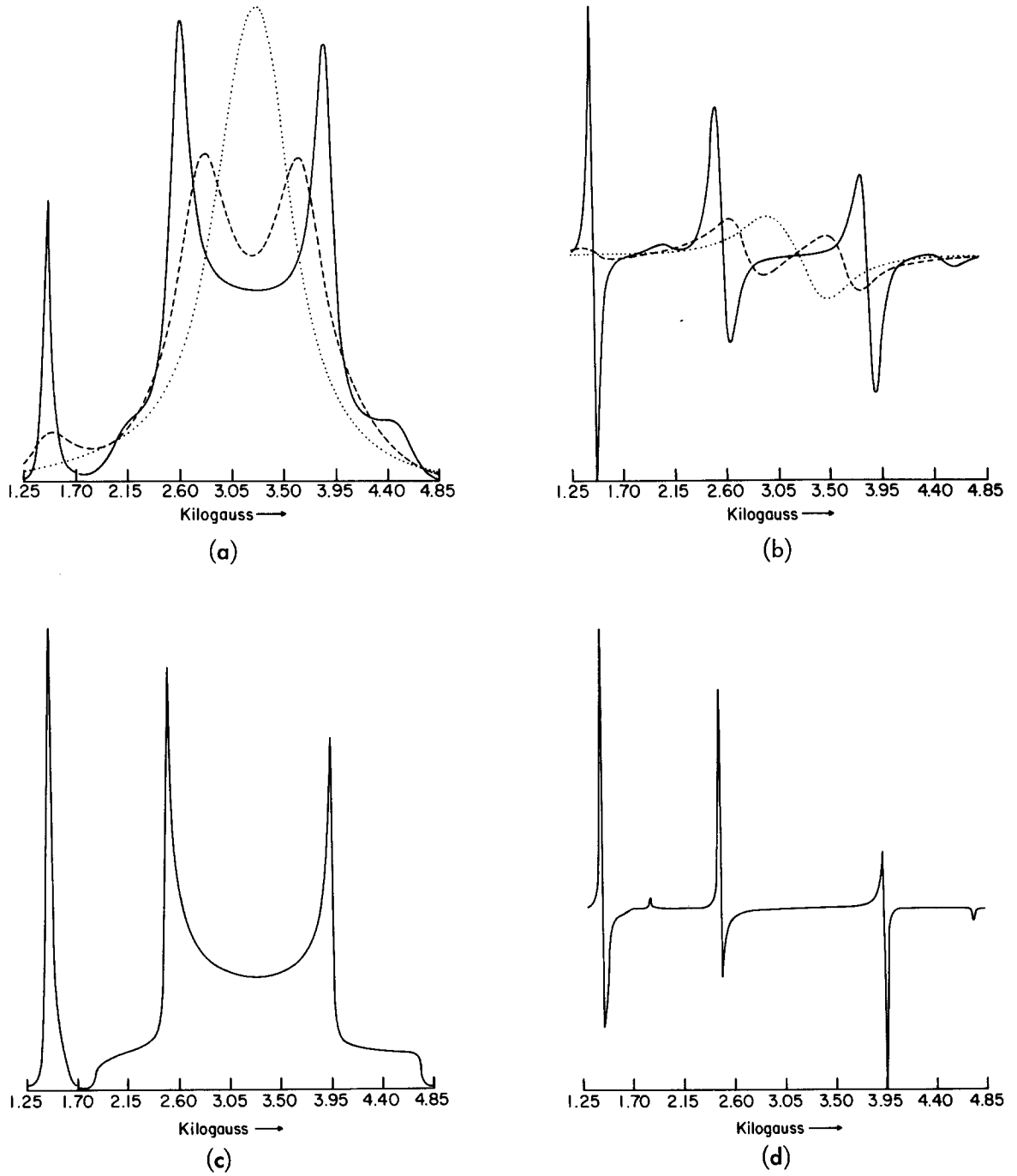

FIG. 1. Line shapes as a function of D/R for a triplet with B_1 perpendicular to B_0. (a) Absorption line shapes. (b) First derivative line shapes. The different lines correspond to $\cdots$, $D/R=5$; $n=6$; - - -, $D/R=20$, $n=8$; —, $D/R=200$, $n=12$. (c) and (d) Rigid limit absorption and first derivative line shapes. All plots are for $D=1\,435$ G, $\omega/|\gamma_e|=3\,300$ G, a rotationally invariant $\sqrt{3}T_2^{-1}/2|\gamma_e|=15$ G and $E=0$. The field B_0 is swept.

the motion becomes rapid, one finds that for $B_1 \perp B_0$ a Zeeman line appears at $\omega \sim \omega_0 = 300$ G$\times|\gamma_e|$, while there is a negligible contribution in the region of $\omega \sim D$. In fact, in the motional narrowing region, the width of the Zeeman line is found to be given by Eq. (32), as expected. [More precisely, the Lorentzian width of Eq. (32) is for $\chi''(\omega)/\omega$, cf. Eq. (1).] This, then, is a simple example of a more general phenomenon: that if,

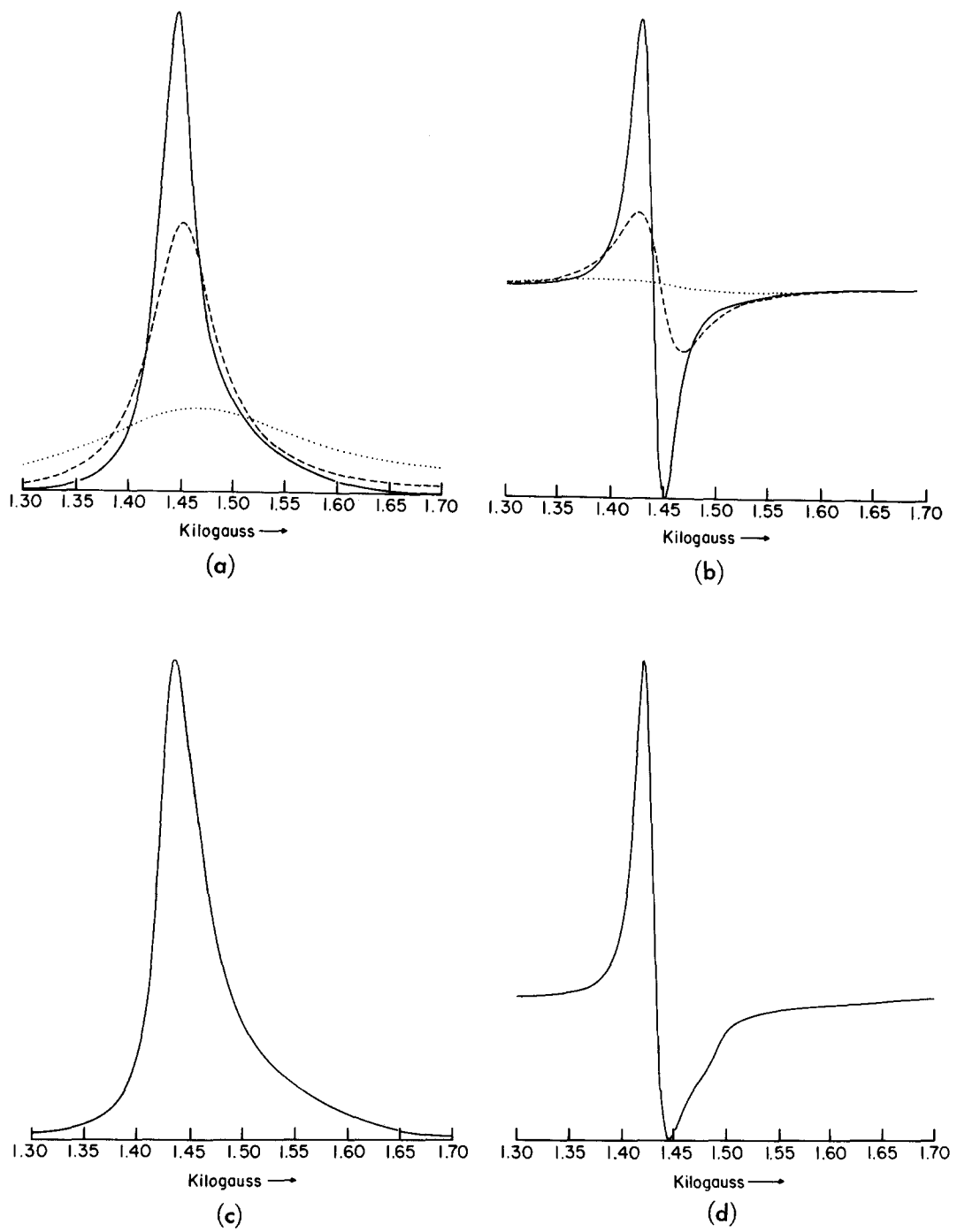

FIG. 2. Half-field line shapes as a function of D/R for a triplet with B_1 perpendicular to B_0. (a) absorption line shapes. (b) First derivative line shapes. The different lines correspond to: ····, $D/R=40$; $n=8$; - - - -, $D/R=200$, $n=12$; —, $D/R=1000$, $n=16$. Other details as given in Fig. 1.

in the rigid limit, the spins are quantized essentially in a molecular frame (the Zeeman field is only a perturbation), they will nevertheless appear to be quantized in the laboratory frame yielding the usual Zeeman line, when the tumbling rate of the molecule is fast compared to zero-field splittings.

In the case of $B_1 \parallel B_0$, a Zeeman line cannot appear. Instead, a line appears at $\omega=0$ with width predicted by

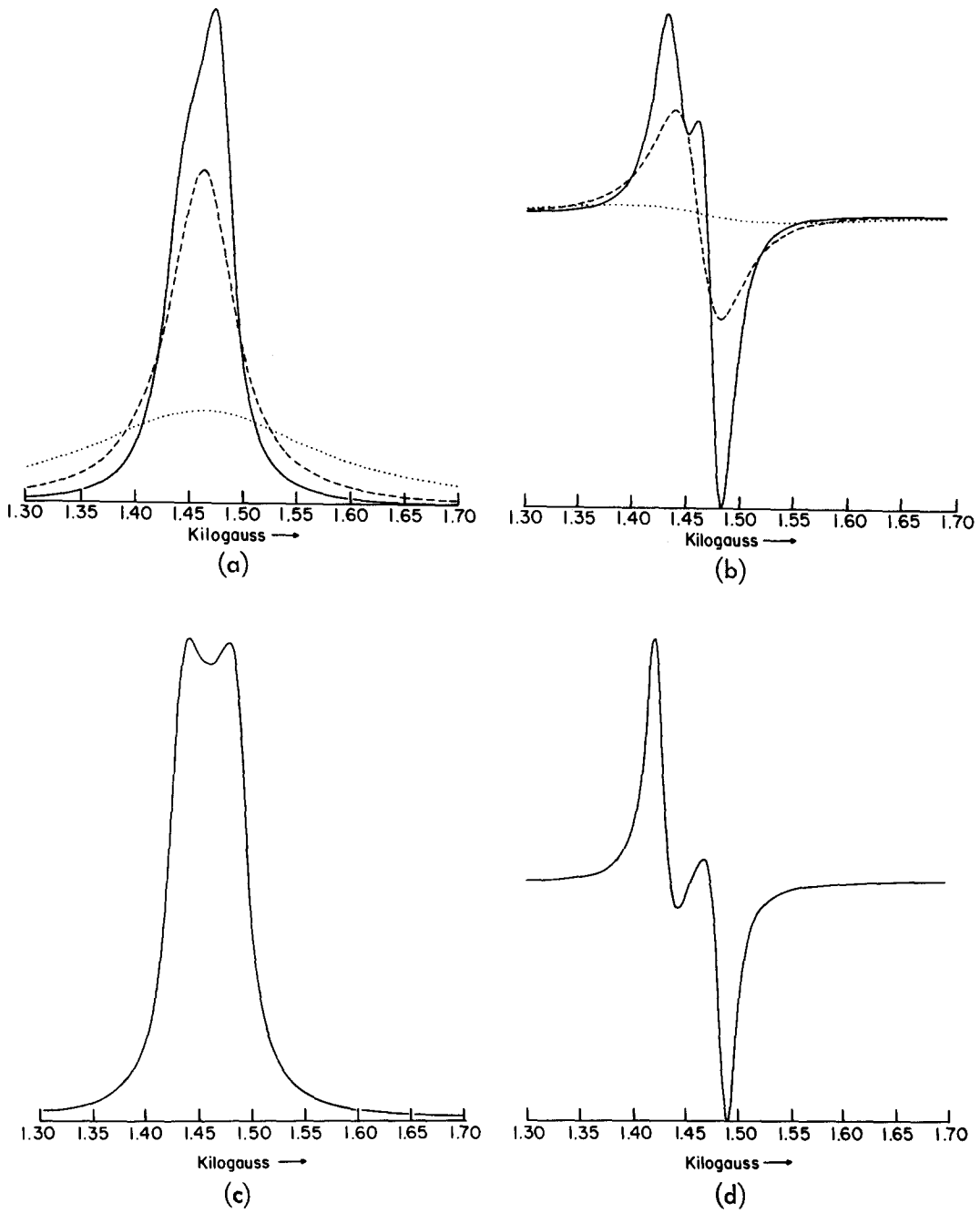

FIG. 3. Half-field line shapes as a function of D/R for a triplet with B_1 parallel to B_0. Details as given in Fig. 2.

Eq. (32). This line would have been apparent in Fig. 5 had we plotted $\chi''(\omega)/\omega$ instead of $\chi''(\omega)$. It is seen from Eq. (1) that the latter must go to zero at $\omega=0$. It is also found that, for very slow motion, $\chi''(\omega)/\omega$ shows a resonance at $\omega\sim 0$, which broadens out as does the regular line which occurs around $\omega\sim D$. A similar phenomenon, but for a simple model of a classically resonanting magnetic moment, has been found by Kubo and Toyabe.[4a,18] The equivalent occurs for zero field [case (C)] wherein it is easily understood (see below). In the present case, with a perturbing Zeeman field, the explanation should be essentially the same.

C. Zero Field and Frequency Sweep

The results for this case are qualitatively similar to Fig. 5 for $B_1 \parallel B_0$ and low fields.

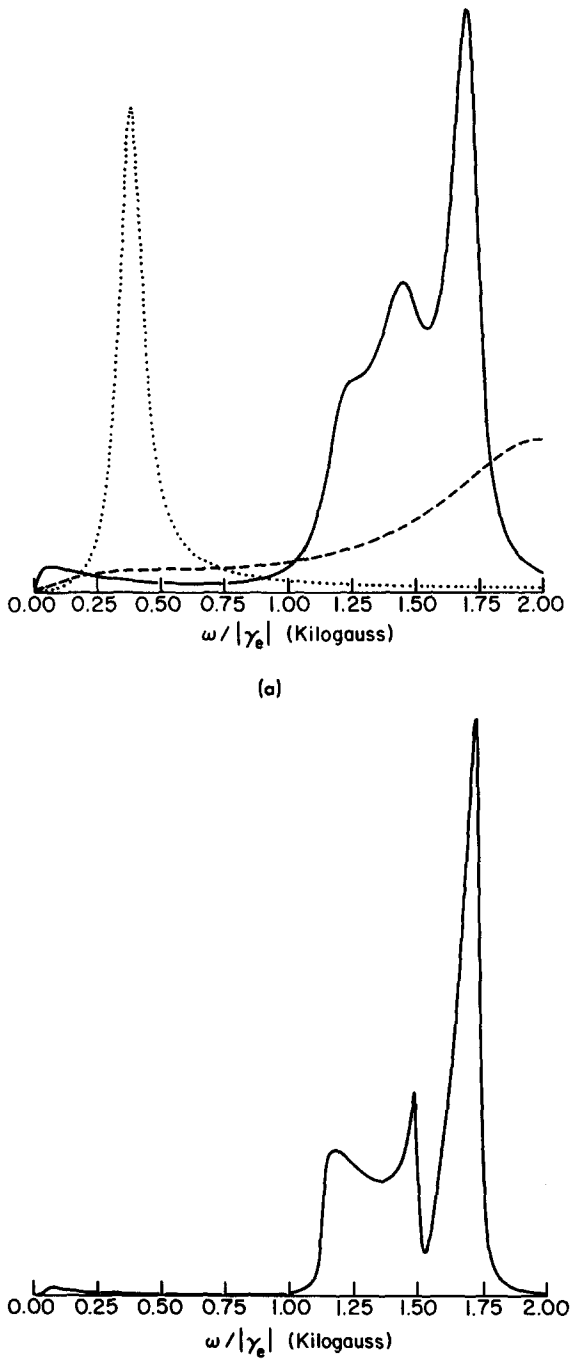

FIG. 4. Low-field absorption line shapes as a function of D/R for a triplet with B_1 perpendicular to B_0. (a) The different lines correspond to ·····, $D/R=0.2$, $n=2$; - - -, $D/R=20$, $n=8$; —, $D/R=200$, $n=12$. (b) Rigid limit. All plots are for $D=1435$ G, $B_0=300$ G, and $T_2^{-1}/|\gamma_e| = (2/\sqrt{3})$ 15 G. The frequency, $\omega = |\gamma_e| B$, is swept.

An analysis of $\chi''(\omega)/\omega$ shows two lines of equal intensity at $\omega=D$ and $\omega=0$, for the rigid limit and for slow motion. These lines are found to be Lorentzian in shape with T_2^{-1} given by $T_2^{-1}=4R$ for $D/6R\gg1$. They correspond to the doubly degenerate $T_x\leftrightarrow T_z$ and $T_y\leftrightarrow T_z$ transitions occurring at $\omega=\pm D$ and to the $T_x\leftrightarrow T_y$ transition at $\omega=0$. Here T_x, T_y, and T_z are the standard zero-field triplet wavefunctions with zero-field energies of D, D, and 0, respectively. For fast motion, a line

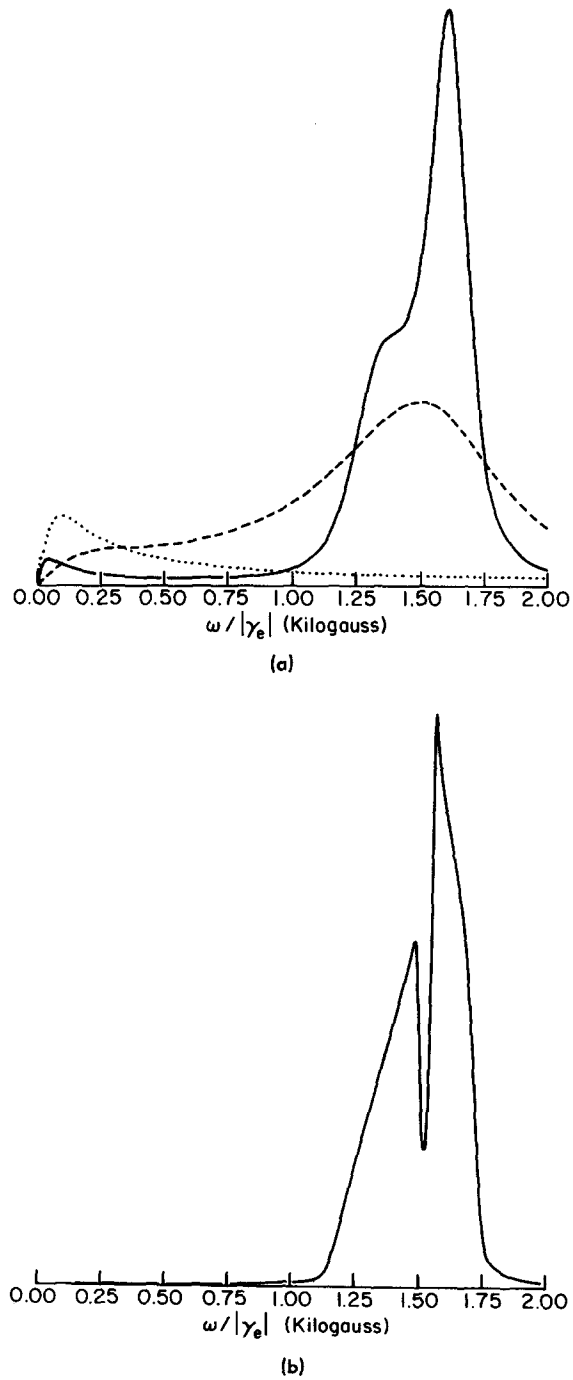

FIG. 5. Low-field absorption line shapes as a function of D/R for a triplet with B_1 parallel to B_0. Details as given in Fig. 4, except ····· is for $D/R=5$, $n=4$.

narrows up at $\omega=0$, with width as predicted by Eq. (32). Of course, the $\omega=0$ lines are suppressed since $\chi''(\omega)$ is studied in a real experiment, rather than $\chi''(\omega)/\omega$.

IV. SUMMARY

General expressions have been obtained which cover a wide range of possible experimental situations associated with the unsaturated ESR line shapes for triplets undergoing rotational reorientation. These include high-, low-, and zero-field resonance spectra, large or small values of the zero field splitting, and slow through fast rotational reorientation. In the present computer simulations, an axially symmetric zero-field splitting was utilized, but the simulations may be extended to more general cases where $E\neq 0$, for which the general expressions have also been obtained.[12]

It is also readily possible to extend the present formulation to cover modes of rotational reorientation other than isotropic rotational diffusion. That is, the possibilities of jump diffusional models or of free diffusion involving inertial effects may be studied by minor modifications of the expressions given here.[10] Also, the effects of anisotropic reorientation[9] may be conveniently introduced.[3,10]

In view of the fact that the rotational motion has been found to have quite different effects on different types of triplet ESR spectra, one may anticipate that a comparison of the range of spectra one can obtain experimentally would offer information that is very sensitive to the precise rate and nature of the rotational motion. Thus, for example, in high field cases, the $\Delta m=1$ transition is largely quantized in the molecular frame, and we obtain the expected sequence as the motion increases, viz., initially a broadening of the rigid spectrum until roughly $D/6R\sim 1$, whereupon the spectrum narrows to the usual Lorentzian. Meanwhile, the $\Delta m=2$ transition continues to broaden out with a width contribution of $6R$, as a simple consequence of the orientation dependence of its transition moment. In the zero-field limit where the spins are quantized in the molecular frame, the slow tumbling motion merely broadens the line(s) by a width contribution found to be just $4R$. The case for weak fields involves an intermediate and more complex description between the high-fields and zero-field cases.

We also note that the results obtained here are quite appropriate for quadrupole resonance spectroscopy for $I=1$ nuclei by replacing the zero-field triplet term by the quadrupole interaction. However, the smallness of the latter would mean that relatively much smaller values of R could be studied in this manner.

ACKNOWLEDGMENT

We wish to acknowledge helpful discussions with Professor S. I. Weissman.

* Supported in part by the Advanced Research Projects Agency and by a grant from the National Science Foundation (Grant No. GP-13780).

† National Institutes of Health Predoctoral Fellow 1969–1971.

[1] J. R. Norris and S. I. Weissman, J. Phys. Chem. **73,** 3119 (1969).

[2] H. Sillescu, J. Chem. Phys. **54,** 2110 (1971).

[3] J. H. Freed, G. V. Bruno, and C. Polnaszek, Abstracts Second Symposium on Electron-Spin Resonance, Athens, Ga., December 1970; J. Phys. Chem. (to be published). Hereafter referred to as I.

[4] R. Kubo, (a) Advan. Chem. Phys. **16,** 101 (1969); (b) J. Phys. Soc. Japan **26,** Suppl. 1, (1969).

[5] F. Bloch, Phys. Rev. **105,** 1206 (1957).

[6] A. Abragam, *The Principles of Nuclear Magnetism* (Oxford U. P., London, 1961) Chaps. III and XII.

[7] A. Abragam in Ref. 6, Chap. IV.

[8] R. Kubo and K. Tomita, J. Phys. Soc. Japan **9,** 888 (1954).

[9] J. H. Freed, J. Chem. Phys. **41,** 2077 (1964).

[10] S. Goldman, G. V. Bruno, C. Polnaszek, and J. H. Freed, "ESR Study of Anisotropic Rotational Reorientation and Slow Tumbling in Liquid and Frozen Media," J. Chem. Phys. (to be published). The effects of reorientational motion other than diffusive are also considered in this work on a doublet free radical.

[11] The modified coefficients $C_{KM}{}^{L}(\pm\omega)$ are introduced in this way to correspond with the coefficients as used in I in the expansion of the density matrix rather than the magnetization. The change of sign in defining $C_{KM}{}^{L}(-\omega)$ as compared to $C_{KM}{}^{L}(\omega)$ does *not* correspond to the usage in I, unless their Eq. (16) and all those which follow have $q\omega_\lambda d_\lambda$ replaced by $q\omega d_\lambda$, i.e., the modified form required for a Bloch–Redfield type approach to yield the correct dependence of $\chi''(\omega)$ on ω as obtained naturally from linear response theory. Note that the equivalent of Eq. (14′) becomes

$$C_m(\omega) = -C_m\dagger(-\omega)N_m{}^{-1}\sum_{m'}\int d\Omega G_m{}^{*}(\Omega)G_{m'}{}^{*}(\Omega).$$

A redefined $C_m'(-\omega)=-C_m(-\omega)$ would thus correspond to the exact usage in I.

[12] G. V. Bruno and J. H. Freed (unpublished).

[13] In this perturbation analysis, one may neglect off-diagonal elements in spin space of the operator Γ, which arise because of the weak orientation dependence of $|\pm'\rangle$, cf. H. Sillescu and D. Kivelson, J. Chem. Phys. **48,** 3493 (1968).

[14] D. Kivelson, J. Chem. Phys. **33,** 1094 (1960); A. D. McLachlan, Proc. Roy. Soc. (London) **A280,** 271 (1964).

[15] P. Kottis and R. Lefebvre, J. Chem. Phys. **39,** 393 (1963); *ibid.* **41,** 379 (1964).

[16] E. Wasserman, L. C. Snyder, and W. A. Yager, J. Chem. Phys. **41,** 1763 (1964).

[17] A. R. Edmonds, *Angular Momentum in Quantum Mechanics* (Princeton U. P., Princeton, N.J., 1957).

[18] R. Kubo and T. Toyabe, Colloq. AMPERE **14,** (1965), 785 (1966).